

## Utilization of Nickel-Modified Natural Zeolite in Catalytic Structural Reforming of Iraqi Naphtha

Mohsen Ismael Khalil <sup>\*1</sup>, Ragheed Yousif Ghazal <sup>\*2</sup>, Nabeel Jamal Ayed <sup>\*3</sup>

1,3 Department of Chemistry, College of Education for pure Science, University of Tikrit, Iraq

2 Department of Chemistry, College of Education for pure Science, University of Mosul, Iraq

E-mail: 1Mohsen.i.khalil@st.tu.edu.iq, 2ragheedghazal76@uomosul.edu.iq, 3dr.nabeel1956@tu.edu.iq

### Abstract:

This research focuses on the utilization of abundant natural mineral resources in Iraq to prepare both unmodified natural zeolite and nickel-modified zeolite. These zeolites are employed in the catalytic thermal structural reforming process of naphtha distillates (35-200°C) under initial temperature conditions (100, 150, 200, 250, 300, 350°C) using a constant catalyst ratio. The zeolites, prepared in two forms, (1)% by weight, and with a reaction time of one hour, were first tested to determine the optimal temperature. Subsequently, the catalyst ratio and reaction time were adjusted based on the initial conditions for each catalyst, to establish the optimum conditions for unmodified zeolite at a temperature of 350°C, a catalyst ratio of (3%), and a reaction time of (3 hours). For nickel-modified zeolite, the optimal conditions were found to be a temperature of 300°C, a catalyst ratio of (3%), and a reaction time of (3 hours). The catalysts exhibited the ability to form rings and facilitate hydrogenation reactions, resulting in the preparation of aromatic compounds that reached threefold their original concentration. Specifically, the concentration increased from (7.1%) to (23.61%) in the nickel-modified catalyst. These results were determined through techniques such as Nuclear Magnetic Resonance (1HNMR) spectroscopy, Gas Chromatography-Mass Spectrometry (GC/MS), and Infrared Spectroscopy (IR).

**Keywords:** Natural zeolite, Iraqi naphtha, catalytic structural reform.

### تحضير زيولايت طبيعي من خام طيني معدني وتطعيمه بالكروم ودراسة خصائصه الحفازية

<sup>\*1</sup> محسن اسماعيل خليل ، <sup>\*2</sup> رغيد يوسف غزال ، <sup>\*3</sup> نبيل جمال عائد

<sup>3.1</sup> قسم الكيمياء - كلية التربية للعلوم الصرفة - جامعة تكريت/ العراق

<sup>2</sup> قسم الكيمياء - كلية التربية للعلوم الصرفة - جامعة الموصل/ العراق

### مستخلص:

يتضمن البحث دراسة أحد الخامات المعدنية الطينية الطبيعية المتواجدة في منطقة النمرود/ قرية الياجور (40 كم جنوب شرق مدينة الموصل) عن طريق التحليل الكيميائي للخام وفلورة الأشعة السينية (XRF) للتعرف على مكوناته من العناصر المختلفة ثم دراسة حيود الأشعة السينية (XRD) لمعرفة النسب المثوية للمعادن الطينية الزيولايتات الطبيعية (المونتمورلونيت والكائولين) وغير الطينية (الكوارتز والكالسايت) المكونة للخام المعدني الطبيعي، بعدها يُنقى ويُركز الزيولايت الطبيعي من خلال إزالة الكربونات والحديد والسيليكا غير البلورية (amorphous) ثم يُطعم بعنصر الكروم باستخدام المركب كلوريد الكروم ( $CrCl_3 \cdot 6H_2O$ )، دُرست بعدها خصائص ومواصفات الزيولايتات المُحضرة (المُطعم بالكروم وغير المطعم) باستخدام تقنيات (XRF) و (XRD) و (BET) و (SEM) فضلا عن التحليل الحراري الوزني (TGA) وتبين احتواءه على تركيب كيميائي وبلوري ضمن مواصفات الزيولايت فضلا عن المساحة السطحية والقنوات المسامية الانتقائية والاستقرار الحراري الجيد.

الكلمات المفتاحية: الزيولايت الطبيعي المُطعم بالكروم، المونتمورلونيت، المجهر الإلكتروني الماسح، فلورة الأشعة السينية، التحليل الحراري الوزني.

## 1. Introduction:

Catalysts are chemical substances introduced into a chemical reaction medium to enhance the rate of chemical reaction thermodynamically feasible, providing an alternative reaction pathway by lowering the activation energy barrier [1]. Catalysts are not consumed during the reaction and can be recovered at the end of the process for reuse, although they may sometimes require regeneration prior to reuse [2]. Catalysts can be broadly categorized into three types: Homogeneous Catalysts: These catalysts are in the same phase as the reactants and products [3]. Heterogeneous Catalysts: These catalysts are in a different phase from the reactants and products. Biocatalysts: These catalysts involve enzymatic processes, stimulating diverse biochemical reactions within organisms [4]. Zeolite is a type of heterogeneous catalyst subject to ongoing global research. Chemically, zeolite is composed of hydrated aluminosilicate, crystalline solids with intricate microporous frameworks possessing channels, voids, and molecular-sized windows [5]. Zeolite structures consist of an infinite number of tetrahedral ( $TO_4$ ) units, where the tetrahe-

dral (T) atom can be various combinations of elements such as (Si, Al), (Si, B), (Si, Ga), and more [6]. Basic zeolite structures consist of an internal porous system with interconnected voids resembling cages or a unified channel system [7]. Zeolite types can be classified based on pore size or diameter: Zeolites with Small Pores (eight-membered ring pores) and free pores with a diameter of 0.3-0.45 nanometers (e.g., Zeolite A) [8]. Zeolites with Medium Pores (ten-membered ring pores) and free pores with a diameter of 0.45-0.6 nanometers (e.g., Zeolite ZSM-5) [9]. Zeolites with Large Pores (twelve-membered ring pores) and free pores with a diameter of 0.6-0.8 nanometers (e.g., Mordenite, Beta, Y). Zeolites with Very Large Pores (fourteen-membered ring pores) and free pores with a diameter of 0.8-1.0 nanometers (e.g., VTD-1) [10]. Certain zeolite types, such as those with medium-sized pores, possess pores with diameters of a few nanometers [11]. The International Zeolite Association (IZA) has registered around 130 zeolite structures of molecular sieve types, but only 15 of them have industrial applications [12]. Zeolite finds essential applications in catalyzing the conversion of

heavy petroleum derivatives into more valuable products like gasoline and kerosene [13]. Zeolite catalyzes various reactions such as hydrogenation, isomerization, cyclization, and hydrogen removal, with catalytic cracking being a major application, producing over 500 million tons annually worldwide [14]. Flanigen's classification categorizes zeolite types according to their silica-to-alumina ratio and development [15]: Low-Silica or Al-Rich Zeolite, Medium Silica Zeolite, High-Silica Zeolites. Naphtha is a highly flammable, light hydrocarbon mixture derived from coal distillation, oil refining, or shale gas processing [16]. It encompasses petroleum derivatives with boiling points typically ranging from 200°C to 30°C, primarily represented by hydrocarbons (C10-C5) [17]. Zeolite (ZSM-5) has been used to crack naphtha, producing light olefins [13]. Naphtha serves as a leading product in refineries, utilized in various industries as feedstock, gasoline blend, solvent, and fuel due to its high energy content and clean-burning properties. Zeolite catalysts play a pivotal role in naphtha conversion processes, enhancing selectivity and stability [18]. Ongoing research continues to refine zeolite ap-

plications in this context [19].

## 2. Practical part

### 2.1. Chemicals used:

Nickel Nitrate ( $\text{NiNO}_3 \cdot 6\text{H}_2\text{O}$ ) (BDH), Deionized water, (prepared zeolite from previous research) were used in this study.

### 2.2. Preparation of Catalysts (Nickel-Loaded and Unloaded Zeolite):

The catalyst (zeolite) is synthesized from naturally abundant mineral ore found in Iraq, possessing suitable proportions of silica and alumina  $\text{Si}/\text{Al}=3$  it can be classified to faujasite type Y zeolite. The raw material is sourced from the Nimrud region, specifically Ibrahim Al-Khalil village, situated 40 km southeast of Mosul city. After eliminating undesired components, such as carbonates, iron, and amorphous silica that removed by HCl(10%), oxalic acid (3%) and NaOH(0.5M) respectively in previous research. The natural zeolite is obtained. This zeolite will be subsequently employed for the preparation of catalysts impregnated with transitional metal oxides (nickel). In this study, nickel nitrate salt ( $\text{Ni}(\text{NO}_3)_2 \cdot 6\text{H}_2\text{O}$ ) is utilized [20, 21]. To characterize the prepared zeolites, various measure-

ments are conducted, including X-ray fluorescence (XRF), X-ray diffraction (XRD), infrared spectroscopy (IR), Brunauer-Emmett-Teller (BET) analysis, scanning electron microscopy (SEM), and thermogravimetric analysis (TGA).

### 2.3. General Specifications of the Prepared Catalyst (Zeolite):

The specifications and characteristics of the employed catalysts are elucidated based on the measurements performed, as shown in Table 1.

**Table 1. Properties and specifications of refined natural zeolite.**

Measurements and properties	Analysis Data
BET Surface Area	27.2416 m <sup>2</sup> /gm
Langmuir Surface Area	419.4083 m <sup>2</sup> /g
Pore Volume	0.10817 cm <sup>3</sup> /gm
Pore Size	8.73724 nm
Average Particle Size	220.2516 nm
Natural Zeolite Content (Montmorillonite and Kaolinite)	64.55
SiO <sub>2</sub> /Al <sub>2</sub> O <sub>3</sub>	3.35

### 2.4. Preparation and Conditioning of the Under-Study Naphtha:

The under-study naphtha is sourced from the Qusq oil refinery, located 45

km west of Mosul in Ninawa Governorate. Table 2 details the specifications of the naphtha under study.

**Table 2. Specifications of the naphtha under study.**

Test	Data
Boiling Range	(35-200°C)
Specific gravity at 15°C	0.7271
API	63.108
Density (gm/cm <sup>3</sup> )	0.717
Sulphur Content (Wt.) %	0.166

## 2.5. Implementation of Catalytic Reforming Reactions on the Under-Study Naphtha:

### 2.5.1. Selection of Reaction Conditions:

The initial reaction conditions for the naphtha reforming were chosen as presented in Table 3. Through the use of various techniques, it has been established that the optimal temperature for the initial conditions is 350°C for unloaded zeolite and 300°C for zeolite loaded with nickel. Based on these temperatures, the optimal conditions for catalytic treatment are determined. In our study, catalyst ratios of 1%, 2%, and 3% are used. These ratios are add-

ed to an autoclave reactor along with 100 grams of naphtha [22]. After sealing the reactor, it is agitated and heated to varying temperatures. The reactions are conducted for different time intervals ranging from 1 to 3 hours at each temperature. Upon completion, the reactor is allowed to cool to lab temperature, and the treated liquid material (naphtha) is filtered and stored in dedicated containers for further analysis and measurements [23]. Figure 1 illustrates the autoclave reactor used in the study. Table 4 outlines the optimal conditions employed for the catalytic reforming reaction on the under-study naphtha.

**Table 3. Initial conditions for the synthetic reforming reaction of naphtha**

Circumstances	Value
temperature used	(100, 150, 200, 250, 300, 350) °C
Additive catalyst ratio	1% of the weight of naphtha
transaction time	One hour

## 2.6. Determining the optimal conditions for conducting the catalytic synthetic reforming reactions of naphtha

**Table 4. Optimal conditions for the synthetic reforming reaction of naphtha**

No	Reaction conditions	Value
1	Temperature used	It was found that the best temperature for the un grafted zeolite was (350 °C), while for the grafted zeolite it was (300 °C).
2	The percentage of catalyst added	The catalyst percentage was increased to (2%) and (3%) while it was (1%) in the initial conditions by weight of naphtha.
3	Transaction time	The reaction was carried out with a time of (2 and 3 hours), while it was one hour in the initial conditions.

## 2.7. Analysis of Reforming Reaction Products

### 2.7.1. Fourier Transform Infrared Spectrometer (FTIR)

The infrared spectra of the parent naphtha model, as well as the untreated naphtha samples and the catalyst-treated naphtha samples, were measured using a Spectrophotometry FTIR ATR device (Platinum Braker, Germany). This analysis aimed to identify structural changes in the samples resulting from catalytic treatment and to potentially discover new absorption patterns.

### 2.7.2. Nuclear Magnetic Resonance Spectrometer (<sup>1</sup>H-NMR)

Furthermore, the nuclear magnetic resonance (NMR) spectra of the parent naphtha model and the catalyst-treated naphtha samples were measured using a Varian 500 MHz (1H NMR) device. This analysis aimed to identify the types of protons present in the hydrocarbon compounds of the naphtha, thereby revealing the hydrocarbon molecular structure. The proton and carbon distribution of the treated naphtha samples were subsequently calculated based on this information.

### 2.7.3. GC/MS Measurement For naphtha Samples

Gas chromatography-mass spec-

trometry (GC/MS) technique was employed to identify the types of changes occurring in the hydrocarbon structures of the parent naphtha and the catalyst-treated naphtha, including paraffins, olefins, naphthene, and aromatic compounds collectively known as PONA. The measurements were conducted using an Agilent GC/MS device.

### 2.7.4. Measurement of Density

For each sample, precisely 5 mL of parent naphtha and catalyst-treated naphtha were individually placed in a pre-weighed, dry volumetric flask. The flask weight difference was used to determine the sample weight (given that the flask volume is known), and this weight was used to calculate the density (d) using the following formula:

$$d = w/v, \text{ where: } d = \text{Density (g/cm}^3\text{)}, \\ w = \text{Weight (g)}, v = \text{Volume (cm}^3\text{)}''$$

## 3. Results and Discussion

### 3.1. Infrared Spectroscopy Measurement (FTIR) for Naphtha Samples

Infrared spectroscopy (FTIR) analysis was conducted on the parent naphtha samples (untreated) and the catalyst-treated naphtha samples. The FTIR measurement provides evidence of structural changes occurring in the

reforming reactions of petroleum derivatives (naphtha). These changes may involve the creation of new hydrocarbon compounds such as ring formation and hydrogen removal [24]. In this study, FTIR analysis was carried out to identify structural modifications in the under-study naphtha in the presence of catalysts (nickel-loaded zeolite and unloaded zeolite). The reactions were performed under initial conditions with a fixed time and catalyst ratio (1%) and variable temperatures (100, 150, 200, 250, 300, 350°C) [25]. Subsequently, the reaction time was extended to 2 and 3 hours, and the catalyst ratio was changed to 2% and 3%, while maintaining the optimal temperature for each catalyst. The FTIR analysis revealed the emergence of new changes in the hydrocarbon structure of the naphtha samples. Notably, new absorption peaks appeared in the region of 3000-3100  $\text{cm}^{-1}$  across most samples, with a more pronounced presence in the sample treated with nickel-loaded zeolite at a 1% weight ratio, 1-hour reaction time, and 300°C temperature [26, 27]. This peak is attributed to the aromatic ring's C-H bending vibrations, indicating the formation of these compounds in the reactions. Ad-

ditionally, new absorption peaks in the range of 1450-1600  $\text{cm}^{-1}$  corresponded to the aromatic ring's C=C vibrations and varied based on the concentration of aromatic compounds formed during the reactions. Furthermore, an increase in absorption was observed in the region of 675-800  $\text{cm}^{-1}$ , attributed to out-of-plane bending (scissoring) vibrations of aromatic C-H bonds [28]. The clear emergence of these absorption peaks, especially in samples with evident reforming reactions, is consistent with nuclear magnetic resonance spectroscopy ( $^1\text{H-NMR}$ ) and gas chromatography-mass spectrometry (GC/MS) results. This underscores the catalysts' (zeolites') ability to facilitate these reactions due to their acidic, crystalline, and porous properties.

### 3.2. Measurement of $^1\text{H-NMR}$ Spectroscopy for Naphtha Samples

Treatment of naphtha with various conditions of temperature, reaction time, and catalyst (zeolite) ratio induces structural changes in the hydrocarbon constituents, including paraffins, naphthenes, and aromatics, as well as ring compensation. To understand these changes,  $^1\text{H-NMR}$  spectroscopy is utilized, providing qualitative and quantitative information about the specific

proton types within these compounds. This spectroscopy identifies five major proton sites: methyl protons (H<sub>me</sub>) at 0.5-1.4 ppm, methylene protons (H<sub>my</sub>) at 0.9-1.8 ppm [29], naphthene protons

(H<sub>N</sub>) at 1.4-2.2 ppm [30], alpha protons of aromatic ring (H<sub>α</sub>) at 1.7-3.4 ppm [31], and aromatic protons (H<sub>A</sub>) at 6.3-8.5 ppm [32], as shown in Table 5.

**Table 5. Relative distribution of protons for the treated and untreated naphtha samples measured through <sup>1</sup>H NMR spectroscopy.**

Samples (*)	H <sub>A</sub>	H <sub>α</sub>	H <sub>N</sub>	H <sub>my</sub>	H <sub>me</sub>
1	6.61	7.20	12.98	42.87	30.34
2	11.79	6.92	12.81	40.9	27.58
3	14.08	5.81	11.1	37.3	31.71
4	15.11	5.51	9.5	38.6	31.28
5	18.67	4.90	8.04	36.22	32.17
6	22.72	5.13	4.87	33.02	34.26
7	24.12	6.2	6.69	33.54	29.45

**Where Samples (\*) means:**

- 1: Untreated mother naphtha.
- 2: Naphtha treated with a zeolite catalyst at a temperature of (350°C) for a period of (1 hour) and the catalyst percentage was (1%).
- 3: Naphtha treated with a zeolite catalyst at a temperature of (350°C) for a period of (3 hours) and the catalyst percentage was (2%).
- 4: Naphtha treated with a zeolite catalyst at a temperature of (350°C) for a period of (3 hours) and the catalyst percentage was (3%).:
- 5: Naphtha treated with a nickel-doped zeolite catalyst at a temperature of

(300°C) for a period of (1 hour) and a catalyst percentage of (1%).

- 6: Naphtha treated with a nickel-doped zeolite catalyst at a temperature of (300°C) for a period of (3 hours) and a catalyst percentage of (2%).

- 7: Naphtha treated with a nickel-doped zeolite catalyst at a temperature of (300°C) for a period of (3 hours) and a catalyst ratio of (3%).

Table 5 reveals that the untreated parent naphtha model consists of aromatic compounds at a ratio of 6.61%, naphthenic compounds at 12.98%, and paraffinic compounds (H<sub>my</sub>+H<sub>me</sub>) at 73.21% [33]. The compensatory ring

structure ( $H\alpha$ ) constitutes 7.20% of the composition [34]. Upon treating the naphtha with natural zeolite (unloaded) in models 2, 3, and 4, there is an observed increase in the aromatic compounds, reaching 15.11% in model 4 [35]. Simultaneously, the paraffinic compounds ( $H_{my} + H_{me}$ ) decrease to 69.88%, indicating a process of ring formation from paraffins followed by hydrogen removal [36]. This is corroborated by the presence of aromatic compounds.

Regarding naphtha treated with nickel-loaded zeolite in models 5, 6, and 7 [37], an increase in aromatic compound formation was observed, reaching 24.12% in model 7, accompanied by a decrease in paraffinic compounds to 62.99% [38]. The alpha proton site ( $H\alpha$ ) of the aromatic ring showed a slight decrease, reaching its lowest proportion of 5.13% in model 6, indicative of a dealkylation process of alkyl groups attached to the aromatic ring [39]. As illustrated in Figures 7 and 8, the nuclear magnetic resonance ( $^1H$ -NMR) spectra for the naphtha models further support these observations.

### 3.4. Gas Chromatography-Mass Spectrometry (GC/MS) Analysis for Treated Naphtha Models

This analysis technique is employed to discern hydrocarbon structural changes in naphtha. Gas chromatography separates compounds based on their retention times within the separation column, and mass spectrometry identifies each separated compound's type while determining the area under the peak [40]. This allows us to quantify and identify the types of compounds within the sample, particularly the four main types: paraffinic, olefinic, naphthenic, aromatic compounds (collectively abbreviated as PONA) [41]. These compounds are classified using the first letter of each type. The following table outlines the ratios of these compounds in the untreated parent naphtha and treated models according to the varying conditions of temperature, catalyst ratio, and reaction time.

**Table 6. GC/MS Analysis for Untreated and Treated Naphtha Models.**

Samples (*)	Hydrocarbon Types (PONA)			
	Paraffins%	Olefins%	Naphthenes%	Aromatics%
1	78.8	2.2	11.9	7.1
2	71.8	3.9	11.5	12.8
3	67.6	5.7	10.8	15.9
4	66.3	6.1	10.2	17.4
5	65.13	5.9	9.71	19.26
6	63.12	5.5	9.93	21.45
7	62.48	6.1	7.81	23.61

The table reveals that the untreated parent naphtha, Model (1), contains a high percentage of paraffins, reaching 78.8%, whereas aromatic compounds were found in lower quantities, specifically 7.1%. The naphthenic compounds constituted 11.9%, while the unsaturated paraffinic compounds, namely olefins, accounted for 2.2% [42]. Table (6) illustrates that Models (2, 3, 4), treated with the unmodified zeolite catalyst, underwent a significant change in the aromatic compounds' ratio, increasing to 17.4% compared to the 7.1% in the untreated parent model. There was a distinct decrease in paraffinic compounds, dropping to 66.3% in Model (4), indicating a ring-forming process with hydrogen removal, resulting in an increase in aromatic compounds.

Analyzing the results of naphtha treated with nickel-modified zeolite catalyst [43], represented by Models (5, 6, 7), we observe an elevation in aromatic compounds to 23.61%, accompanied by a reduction in paraffinic compounds [44]. In Model (7), the paraffinic compounds decreased to 62.48% from the 78.8% observed in the untreated parent model [45]. This implies that nickel modification has improved the zeolite's characteristics toward ring formation and hydrogen removal [46], facilitating the production of aromatic compounds.

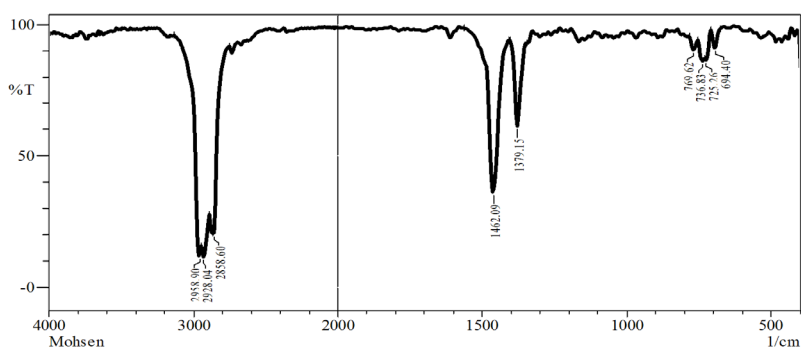
### 3.5. Measured Of density and SP.GR and API

**Table 6. Value Of density and SP.GR and API**

Samples (*)	Density gm/cm <sup>3</sup>	SP.GR	API
1	0.717	0.7271	63.108
2	0.708	0.718	65.575
3	0.7015	0.711	67.515
4	0.7215	0.731	62.070
5	0.7115	0.7216	64.592
6	0.731	0.741	59.458
7	0.7245	0.734	61.279

From Table (6), it is evident that the values of density, specific gravity, and API vary. We observe that the models treated with the same catalyst under different conditions exhibit inconsistent increases and decreases [47]. This variability could be attributed to the pres-

ence of four main types of compounds in the naphtha samples: paraffinic, olefinic, naphthenic, and aromatic compounds [48]. These compounds influence each other's density values, leading to the instability of these measurements.

**Figure 1: The autoclave reactor used in the study.****Figure 2: FTIR spectrum of the parent naphtha**

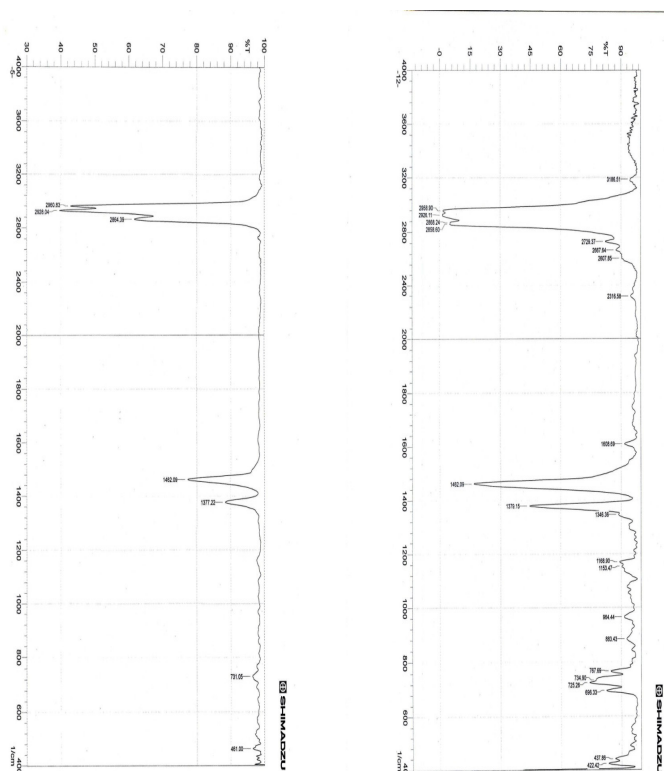


**Figure 3: FTIR spectrum of the naphtha treated at 300°C for 1 hour without catalyst**

**Figure 4: FTIR spectrum of naphtha treated at 350°C for 1 hr. using only natural zeolite 1%**

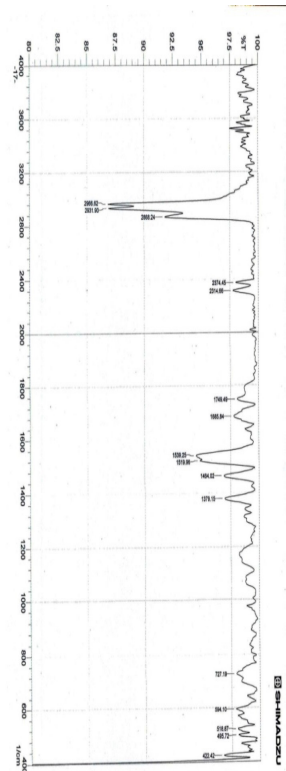


**Figure 5: FTIR spectrum of naphtha treated at 300°C for 1 hr. using Ni-natural zeolite 1%**

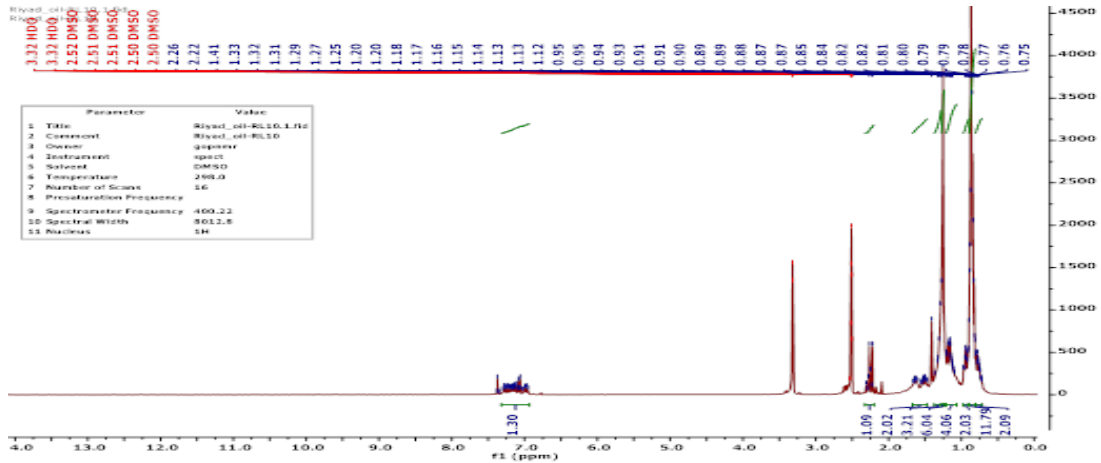


Figure 6:  $^1\text{H}$  NMR spectrum for the untreated parent naphtha model

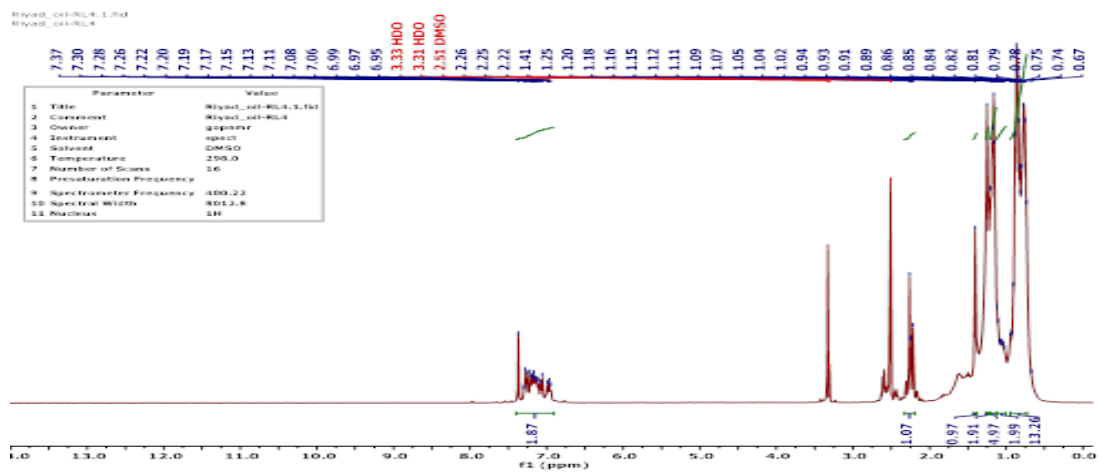


Figure 7:  $^1\text{H}$  NMR spectrum for the naphtha model treated with natural zeolite catalyst at  $350^\circ\text{C}$  for 3 hours with a 3% catalyst ratio

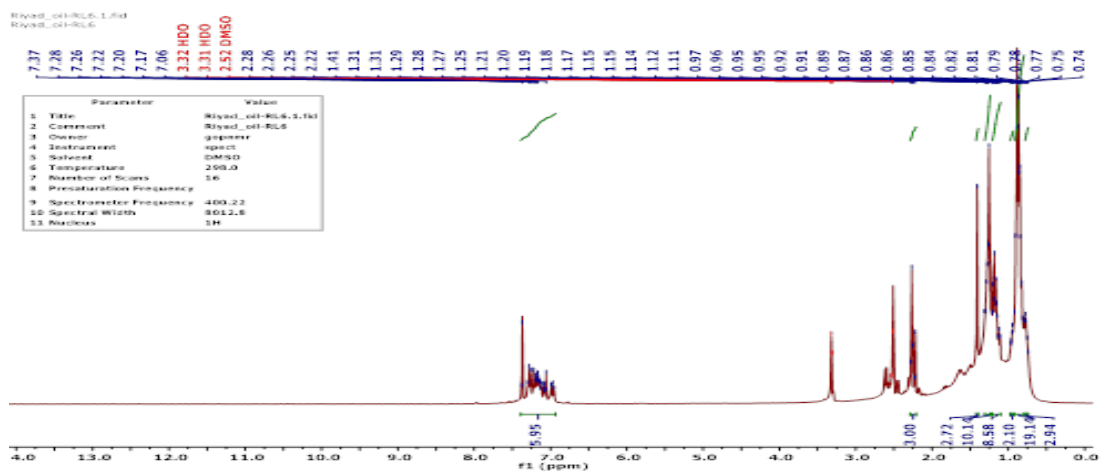
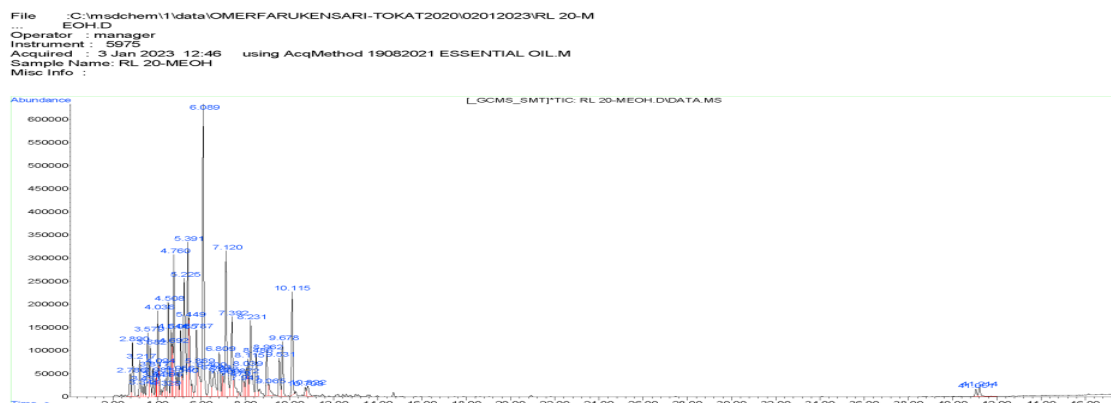
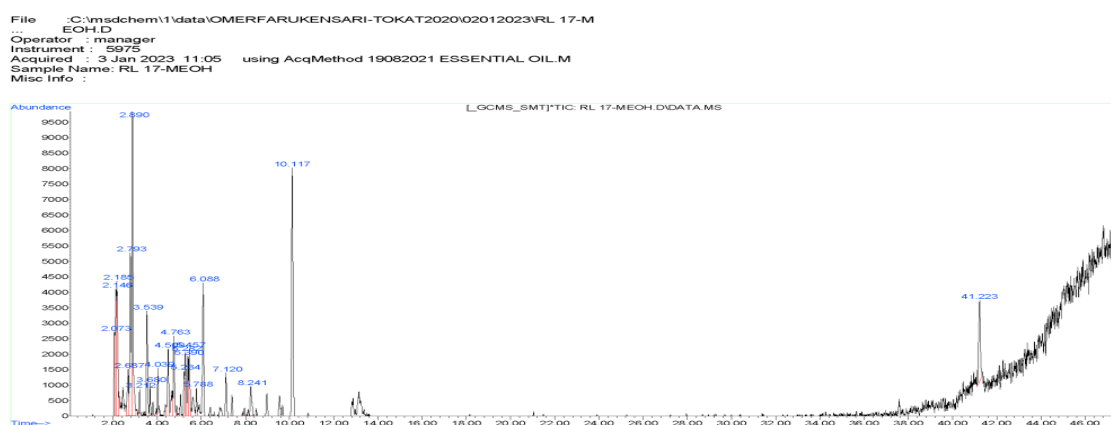


Figure 8:  $^1\text{H}$  NMR spectrum for the naphtha model treated with nickel-loaded natural zeolite catalyst at  $300^\circ\text{C}$  for 3 hours with a 3% catalyst ratio



**Figure 9: GC/MS spectrum of the parent naphtha**



**Figure 10: GC/MS spectrum of Naphtha treated with a nickel-doped zeolite catalyst at a temperature of (300°C) for a period of (3 hours) and a catalyst ratio of (3%).**

#### 4. Conclusion:

The study demonstrated that the purified natural mineral feedstock contains approximately 64.55% of natural zeolite, equivalent to two-thirds of the feedstock's weight. The introduction of transition metal elements (nickel) to the zeolite had a pronounced effect on enhancing the prepared zeolite's

properties. The catalysts prepared using unmodified natural zeolite and nickel-modified zeolite exhibited the capability to form rings and facilitate hydrogen removal to produce aromatic compounds. The aromatic compound content increased threefold to 23.61% after the reaction, compared to the initial content of 7.1% in the nickel-mod-

ified catalyst.

**Acknowledgments:** We extend our gratitude and appreciation to the Deanery of the College of Pure Sciences / Department of Chemistry / University of Tikrit for providing the necessary chemicals and laboratories to fulfill the requirements of this research. Our thanks also go to the Kask Oil Refinery in Nineveh Governorate for supplying us with the parent naphtha.

### References

- Kasula, M. (2020). *Synthesis and catalytic testing of Sn-MFI zeolite crystallized using different tin precursors* (Doctoral dissertation, The Ohio State University).
- Schuring, D. (2002). Diffusion in zeolites: towards a microscopic understanding.
- Mukhopadhyay, A. B. (2004). *Theoretical Investigation of Static and Dynamic Properties of Zeolite ZSM-5 Based Amorphous Material* (Doctoral dissertation, Universität zu Köln).
- Mravec, D., Hudec, J., & Janotka, I. (2005). Some possibilities of catalytic and noncatalytic utilization of zeolites. *Chemical Papers*, 59(1), 62.
- Payra, P., & Dutta, P. K. (2003). Zeolites: a primer. *Handbook of zeolite science and technology*, 2(2), 1-19.
- Klerk, A. D. (2018). Zeolites as catalysts for fuels refining after indirect liquefaction processes. *Molecules*, 23(1), 115.
- Ali, O. M., Alomar, O. R., Ali, O. M., Alwan, N. T., Yaqoob, S. J., Nayyar, A., ... & Abouhawwash, M. (2021). Operating of gasoline engine using naphtha and octane boosters from waste as fuel additives. *Sustainability*, 13(23), 13019.
- Komatsu, T. (2010, December). Catalytic cracking of paraffins on zeolite catalysts for the production of light olefins. In *20th Annual Saudi-Japan Symposium; Catalysts in Petroleum Refining and Petrochemicals, Dharan, Saudi-Arabia*.
- Hsu, C. S., & Robinson, P. R. (Eds.). (2006). *Practical advances in petroleum processing* (Vol. 1, pp. 2334-). New York: Springer.
- Ulmer-Scholle, D. S., Scholle, P. A., Schieber, J., & Raine, R. J. (2014). *A color guide to the petrography of sandstones, siltstones, shales and associated rocks* (Vol. 109). Tulsa,

- OK, USA: American Association of Petroleum Geologists.
- Baba, A. A., Mosobalaje, M. A., Ibrahim, A. S., Girigisu, S., Eletta, O. A., Aluko, F. I., & Adekola, F. A. (2015). BLEACHING OF A NIGERIAN KAOLIN BY OXALIC ACID LEACHING. *Journal of Chemical Technology & Metallurgy*, 50(5).
  - Gougazeh, M. (2018). Removal of iron and titanium contaminants from Jordanian Kaolins by using chemical leaching. *Journal of Taibah University for science*, 12(3), 247-254.
  - Estefan, G., Sommer, R., & Ryan, J. (2013). Methods of soil, plant, and water analysis. *A manual for the West Asia and North Africa region*, 3, 65-119.
  - Karakoulia, S. A., Heracleous, E., & Lappas, A. A. (2020). Mild hydroisomerization of heavy naphtha on mono-and bi-metallic Pt and Ni catalysts supported on Beta zeolite. *Catalysis Today*, 355, 746-756.
  - Son, D. C., Anh, V. T. K., Thom, N. T., Nguyen, H. L. T., Hai, L. V., Thien, C. T., ... & Trang, N. T. T. (2023). Preparation and modification of zeolite A from kaolin for catalytic methanation of carbon dioxide. *Vietnam Journal of Chemistry*, 61(2), 170-177.
  - Guo, Y., Zhang, H., & Liu, Y. (2018). Desorption characteristics and kinetic parameters determination of molecular sieve by thermogravimetric analysis/differential thermogravimetric analysis technique. *Adsorption Science & Technology*, 36(7-8), 1389-1404.
  - Beckhoff, B., Kanngießler, B., Langhoff, N., Wedell, R., & Wolff, H. (Eds.). (2007). *Handbook of practical X-ray fluorescence analysis*. Springer Science & Business Media.
  - Fertey, P. (2017). X-ray Diffraction for Materials Research: From Fundamentals to Applications. By Myeongkyu Lee. CRC Press, 2016. Hardback, pp. 302. Price GBP 99. ISBN 9781771882989. *Acta Crystallographica Section A: Foundations and Advances*, 73(3), 277-278.
  - Naito, M., Yokoyama, T., Hosokawa, K., & Nogi, K. (Eds.). (2018). *Nanoparticle technology handbook*. Elsevier.
  - Condon, J. B., & Area, S. (2006).

- Porosity determinations by physisorption measurements and theory.
- Lee, H. G., Choi, M. K., & Lee, S. C. (2013, September). Grain-oriented segmentation of scanning electron microscope images. In *2013 IEEE International Conference on Image Processing* (pp. 40294033-). IEEE.
  - Brodusch, N., Demers, H., & Gauvin, R. (2018). Imaging with a commercial electron backscatter diffraction (EBSD) camera in a scanning electron microscope: A review. *Journal of Imaging*, 4(7), 88.
  - Dalaf, A. H. (2018). Synthesis and Characterization of Some Quartet and Quinary Hetero cyclic Rings Compounds by Traditional Method and Microwave Routes Method and Evaluation of Their Biological Activity. *M.Sc. Thesis, Tikrit University, Tikrit, Iraq*: 1-94 pp.
  - Dalaf, A. H., & Jumaa, F. H. (2018). Synthesis, Characterization of some 1,3-Oxazepane -4,7-Dione by Traditional and Microwave routes method and evaluation of their biological activity. *Al-utroha for Pure Science*. (8): 93-108.
  - Dalaf, A. H., Jumaa, F. H., & Jabbar, S. A. S. (2018). Synthesis and Characterization of some 2, 3-dihydroquinoxaline and evaluation of their biological activity. *Tikrit Journal of Pure Science*, 23(8): 66-67.
  - Salwa, A. J., Ali, L. H., Adil, H. D., Hossam, S. A. (2020). Synthesis and Characterization of Azetidine and Oxazepine Compounds Using Ethyl-4-((4-Bromo Benzyldiene) Amino) Benzoate as Precursor and Evaluation of Their Biological Activity. *Journal of Education and Scientific Studies*, ISSN: 24134732. 16(5): 39-52.
  - Abd, I. Q., Ibrahim, H. I., Jirjes, H. M., & Dalaf, A. H. (2020). Synthesis and Identification of new compounds have Antioxidant activity Beta-carotene, from Natural Auxin Phenyl Acetic Acid. *Research Journal of Pharmacy and Technology*, 13(1): 40-46.
  - Dalaf, A. H., & Jumaa, F. H. (2020). Synthesis, Identification and Assess the Biological and Laser Efficacy of New Compounds of Azetidine Derived from Benzidine. *Muthanna Journal of Pure Science (MJPS)*, 7(2):12-25.
  - Saleh, R. H., Rashid, W. M., Dalaf, A. H., Al-Badrany, K. A., & Mo-

- ammed, O. A. (2020). Synthesis of Some New Thiazolidinone Compounds Derived from Schiff Bases Compounds and Evaluation of Their Laser and Biological Efficacy. *Ann Trop & Public Health*, **23(7)**: 1012-1031.
- Yass, I. A., Aftan, M. M., Dalaf, A. H., & Jumaa, F. H. (Nov. 2020). Synthesis and Identification of New Derivatives of Bis-1,3-Oxazepene and 1,3-Diazepine and Assess the Biological and Laser Efficacy for Them. *The Second International & The Fourth Scientific Conference of College of Science – Tikrit University*. (P4): 77-87.
  - Salih, B. D., Dalaf, A. H., Alheety, M. A., Rashed, W. M., & Abdullah, I. Q. (2021). Biological activity and laser efficacy of new Co (II), Ni (II), Cu (II), Mn (II) and Zn (II) complexes with phthalic anhydride. *Materials Today: Proceedings*, **43**, 869-874.
  - Aftan, M. M., Jabbar, M. Q., Dalaf, A. H., & Salih, H. K. (2021). Application of biological activity of oxazepine and 2-azetidinone compounds and study of their liquid crystalline behavior. *Materials Today: Proceedings*, **43**, 2040-2050.
  - Aftan, M. M., Talloh, A. A., Dalaf, A. H., & Salih, H. K. (2021). Impact para position on rho value and rate constant and study of liquid crystalline behavior of azo compounds. *Materials Today: Proceedings*.
  - Aftan, M. M., Toma, M. A., Dalaf, A. H., Abdullah, E. Q., & Salih, H. K. (2021). Synthesis and Characterization of New Azo Dyes Based on Thiazole and Assess the Biological and Laser Efficacy for Them and Study their Dyeing Application. *Egyptian Journal of Chemistry*, **64(6)**, 2903-2911.
  - Khalaf, S. D., Ahmed, N. A. A. S., & Dalaf, A. H. (2021). Synthesis, characterization and biological evaluation (antifungal and antibacterial) of new derivatives of indole, benzotriazole and thioacetyl chloride. *Materials Today: Proceedings*.6201-6210 ,(17)47 .
  - Dalaf, A. H., Jumaa, F. H., & Salih, H. K. (2021). Preparation, Characterization, Biological Evaluation and Assess Laser Efficacy for New Derivatives of Imidazolidin-4-one. *International Research Journal of Multidisciplinary Technovation*, **3(4)**, 41-51.

- Dalaf, A. H., Jumaa, F. H., & Salih, H. K. (2021). *MULTIDISCIPLINARY TECHNOVATION. Red*, 15(A2), C44H36N10O8.
- Dalaf, A. H., Jumaa, F. H., Aftana, M. M., Salih, H. K., & Abd, I. Q. (2022). Synthesis, Characterization, Biological Evaluation, and Assessment Laser Efficacy for New Derivatives of Tetrazole. In *Key Engineering Materials* (Vol. 911, pp. 3339-). Trans Tech Publications Ltd.
- Alasadi, Y. Kh., Jumaa, F. H., Dalaf, A. H., Shawkat, S. M., & Mukhlif, M. Gh. (2022). Synthesis, Characterization, and Molecular Docking of New Tetrazole Derivatives as Promising Anticancer Agents. *Journal of Pharmaceutical Negative Results*. 13(3): 513-522.
- Dalaf, A. H., Jumaa, F. H., & Yass, I. A. (2022, November). Synthesis, characterization, biological evaluation, molecular docking, assess laser efficacy, thermal performance and optical stability study for new derivatives of bis-1, 3-oxazepene and 1, 3-diazepine. In *AIP Conference Proceedings* (Vol. 2394, No. 1, p. 040037). AIP Publishing LLC.
- Alasadi, Y. K., Jumaa, F. H., & Dalaf, A. H. (2022, November). Synthesis, identification, antibacterial activity and laser effect of new derivatives of bis-1, 3-oxazepene-4, 7-dione and 1, 3-diazepine-4, 7-dione. In *AIP Conference Proceedings* (Vol. 2394, No. 1, p. 040019). AIP Publishing LLC.
- Toma, M. A., Ibrahim, D. A., Dalaf, A. H., Abdullah, S. Q., Aftan, M. M., & Abdullah, E. Q. (2022, November). Study the adsorption of cyclopentanone on to natural polymers. In *AIP Conference Proceedings* (Vol. 2394, No. 1, p. 040007). AIP Publishing LLC.
- Hamad, A. M., Atiyea, Q. M., Hameed, D. N. A., & Dalaf, A. H. (2023). Green synthesis of copper nanoparticles using strawberry leaves and study of properties, anticancer action, and activity against bacteria isolated from Covid-19 patients. *Karbala International Journal of Modern Science*, 9(1), 12.
- Valle, B., Gayubo, A. G., Aguayo, A. T., Olazar, M., & Bilbao, J. (2010). Selective production of aromatics by crude bio-oil valorization with a nickel-modified HZSM-5 zeolite catalyst. *Energy*

& *Fuels*, 24(3), 2060-2070.

- Wei, L., Kumar, N., Haije, W., Peltonen, J., Peurla, M., Grénman, H., & de Jong, W. (2020). Can bi-functional nickel modified 13X and 5A zeolite catalysts for CO<sub>2</sub> methanation be improved by introducing ruthenium?. *Molecular Catalysis*, 494, 111115.
- Prihadiyono, F. I., Lestari, W. W., Putra, R., Aqna, A. N. L., Cahyani, I. S., & Kadja, G. T. (2022). Heterogeneous catalyst based on nickel modified into Indonesian natural zeolite in green diesel production from crude palm oil. *Int. J. Technol*, 13, 931-943.
- Yao, W., Li, J., Feng, Y., Wang, W., Zhang, X., Chen, Q., ... & Wang, Y. (2015). Thermally stable phosphorus and nickel modified ZSM-5 zeolites for catalytic co-pyrolysis of biomass and plastics. *RSC Advances*, 5(39), 30485-30494.
- Zhou, W., Liu, M., Zhou, Y., Wei, Q., Zhang, Q., Ding, S., ... & You, Q. (2017). 4, 6-Dimethyldibenzothiophene hydrodesulfurization on nickel-modified USY-supported NiMoS catalysts: effects of modification method. *Energy & Fuels*, 31(7), 7445-7455.